Electronic Supplementary Information

A chiral single-component sol-gel platform with highly integrated optical properties

Bin Wu, [a] Hongwei Wu, [b] Yifan Gong, [a] Anze Li, [a] Xiaoyong Jia, *[,c] and Liangliang Zhu*[,a]

[a] State Key Laboratory of Molecular Engineering of Polymers, Department of Macromolecular Science, Fudan University, Shanghai 200433, China

[b] College of Chemistry, Chemical Engineering and Biotechnology, Donghua University, Shanghai 201620, China

[c] Henan Key Laboratory of Photovoltaic Materials, Henan University, Kaifeng 475004, China

Table of Contents

^{1}H, ^{13}C NMR, and MS Spectra for Compounds -- 3

Solvent ratio test between DMSO and toluene for gel formation ------------------------------ 7

FTIR spectra of xerogel of HTB-DG -- 8

XRD pattern of xerogel of HTB-DG --- 8

Time-dependent CD spectra of HTB-D/LG organogel --- 9

AFM images of HTB-DG and HTB-LG xerogels --- 10

TEM images of HTB-DG and HTB-LG xerogels --- 11

Simulation of the length of HTB-D/LG molecule --- 11

UV-Vis and CD spectra of dilute HTB-D/LG solution --- 12

Temperature-dependent CPL and g_{lum} spectra of HTB-DG and HTB-LG ----------------- 13

UV-Vis and CD spectra of HTB-D/LG at 10 mg/mL --- 14

PL, CPL and g_{lum} spectra of HTB-D/LG at 10 mg/mL -- 14

SEM, AFM and TEM images of HTB-D/L xerogels at 10 mg/mL --------------------------- 15

Temperature-dependent PL and lifetime spectra of HTB-DG at 10 mg/mL --------------- 15

Comparison of chiral response with reported literatures -------------------------------------- 16

References -- 17

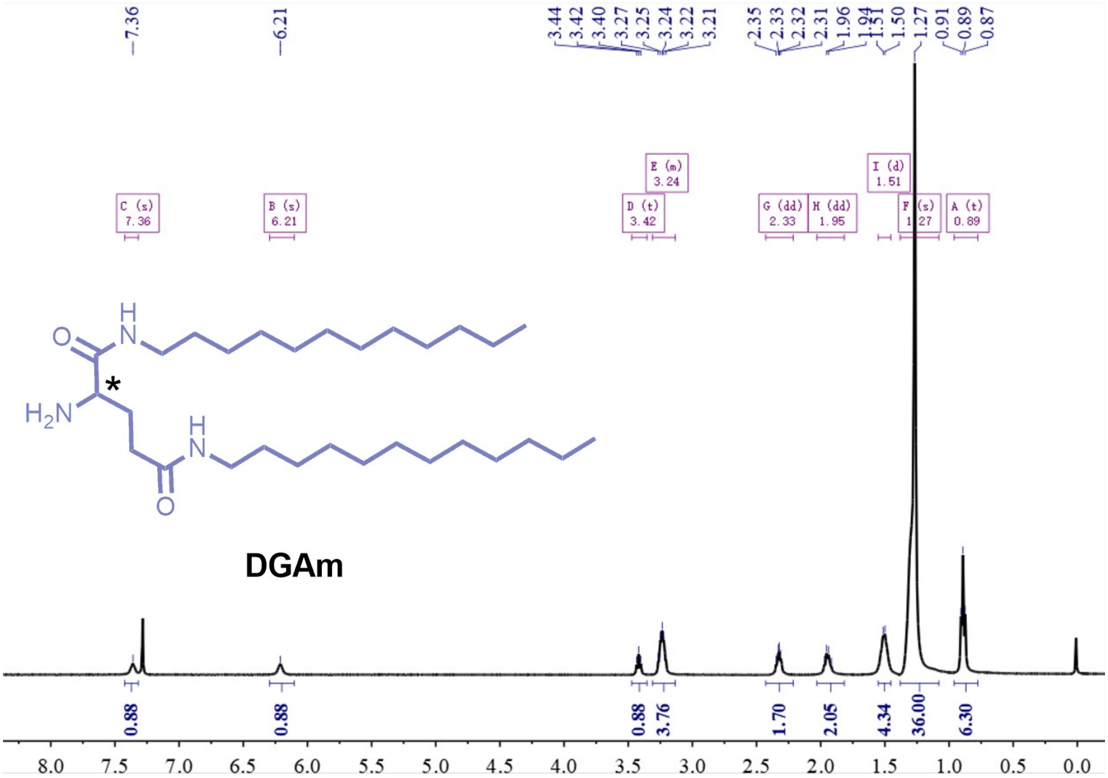

Fig. S1 ^{1}H NMR spectrum for compound **DGAm** ($CDCl_3$, 298 K).

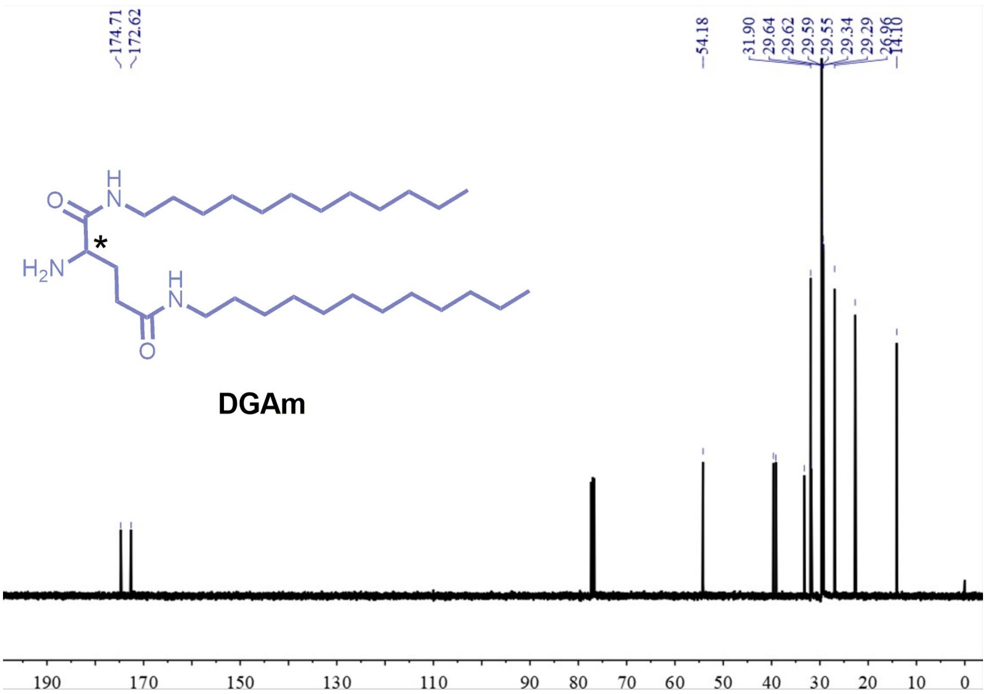

Fig. S2 ^{13}C NMR spectrum for compound **DGAm** ($CDCl_3$, 298 K).

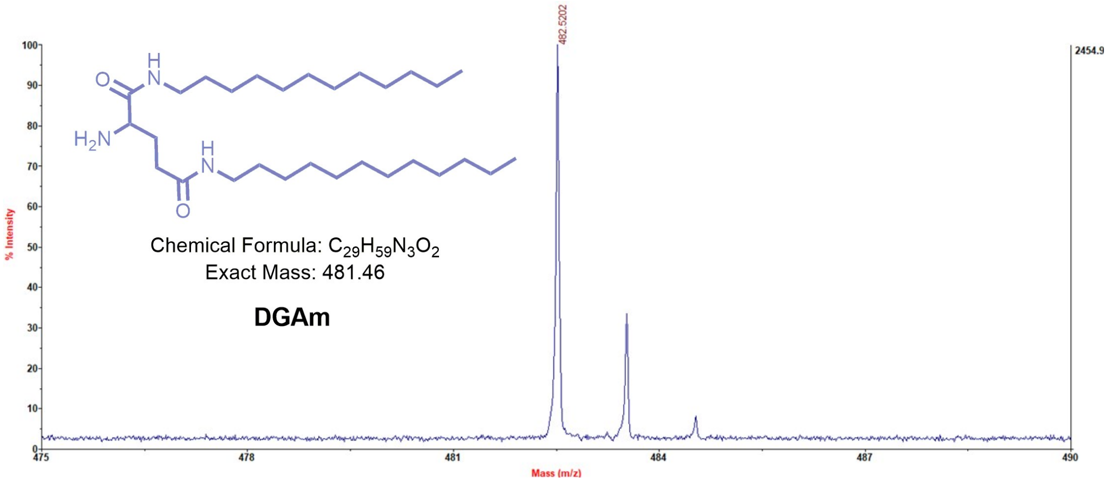

Fig. S3 MALDI-TOF MS Spectrum for compound **DGAm**.

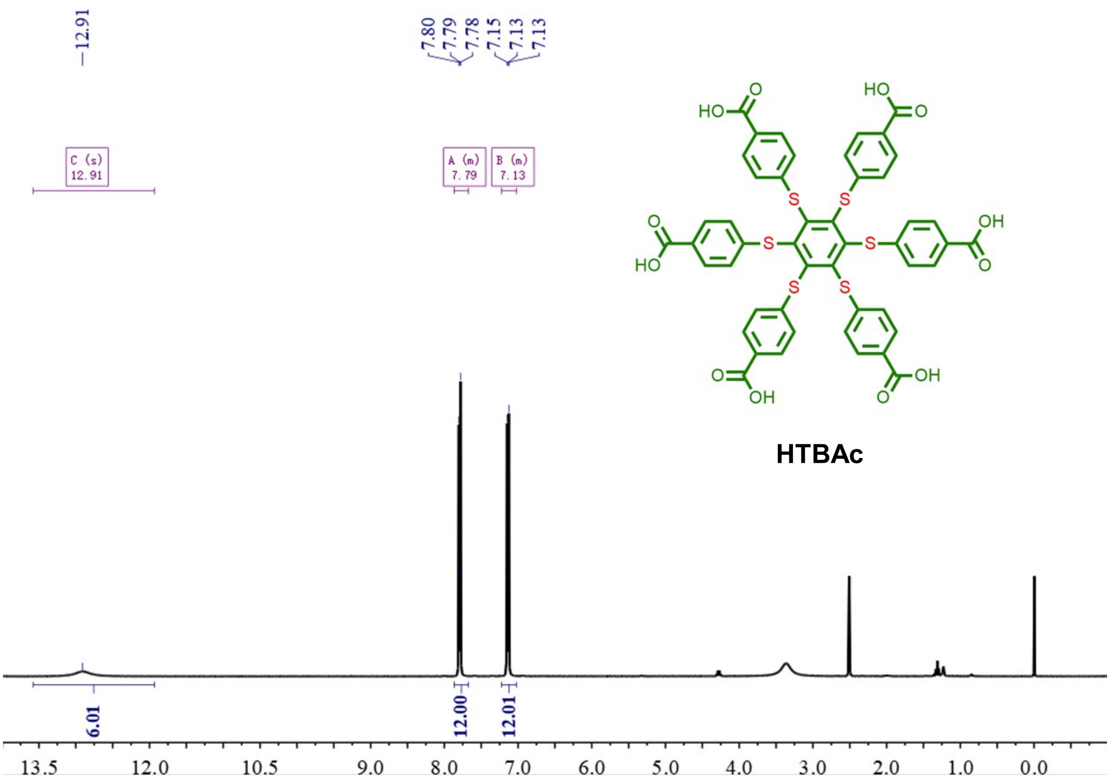

Fig. S4 ^{1}H NMR spectrum for compound **HTBAc** (DMSO-d_6, 298 K).

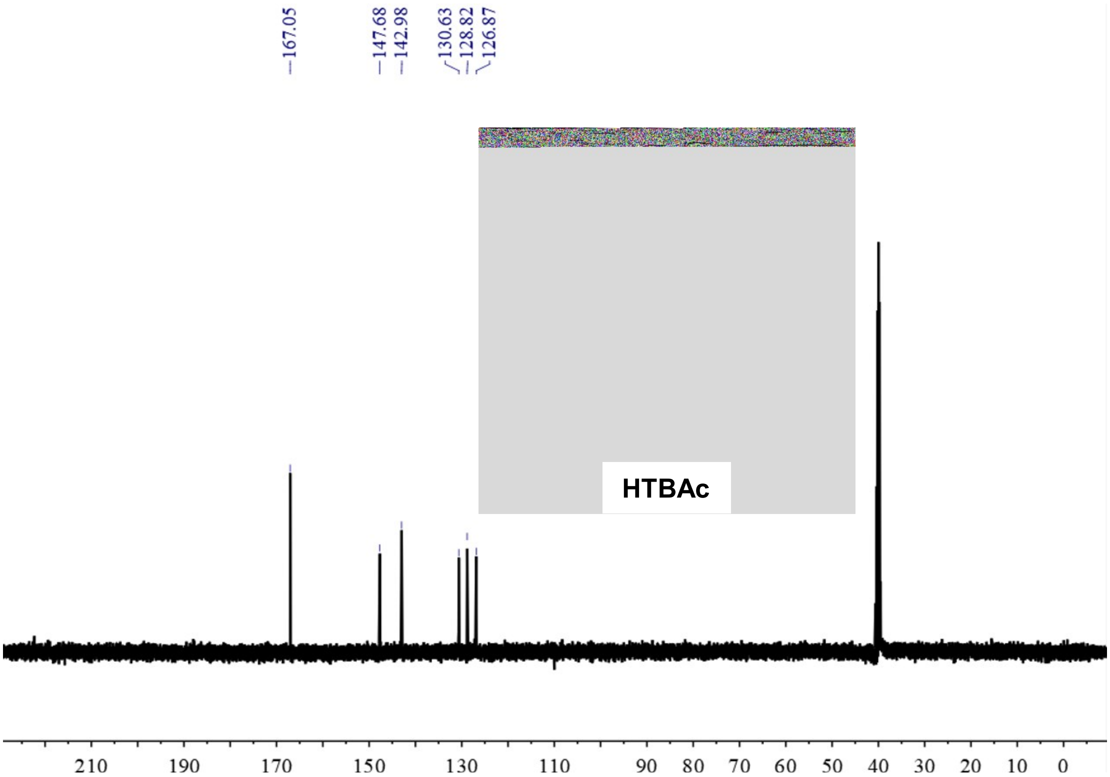

Fig. S5 ^{13}C NMR spectrum for compound **HTBAc** (DMSO-d_6, 298 K).

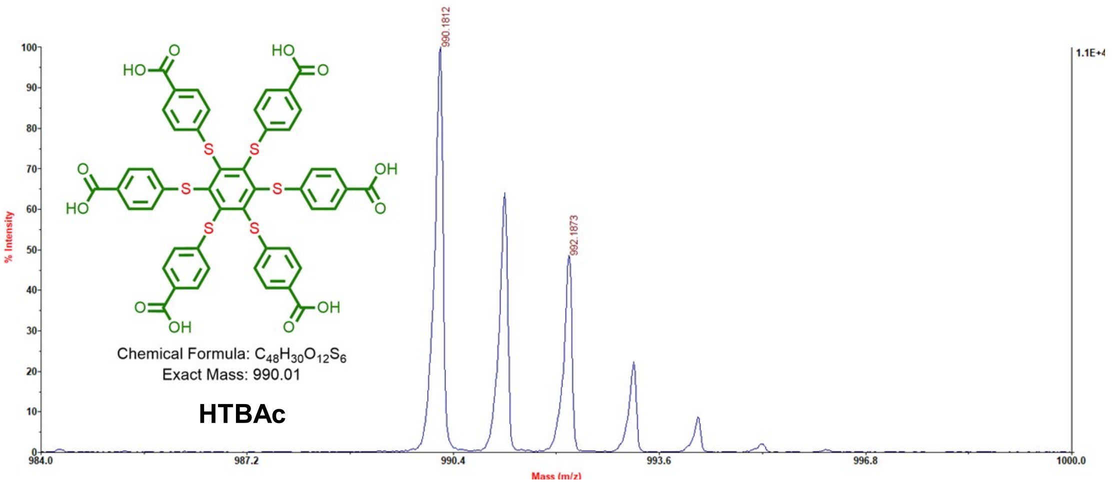

Fig. S6 MALDI-TOF MS Spectrum for compound **HTBAc**.

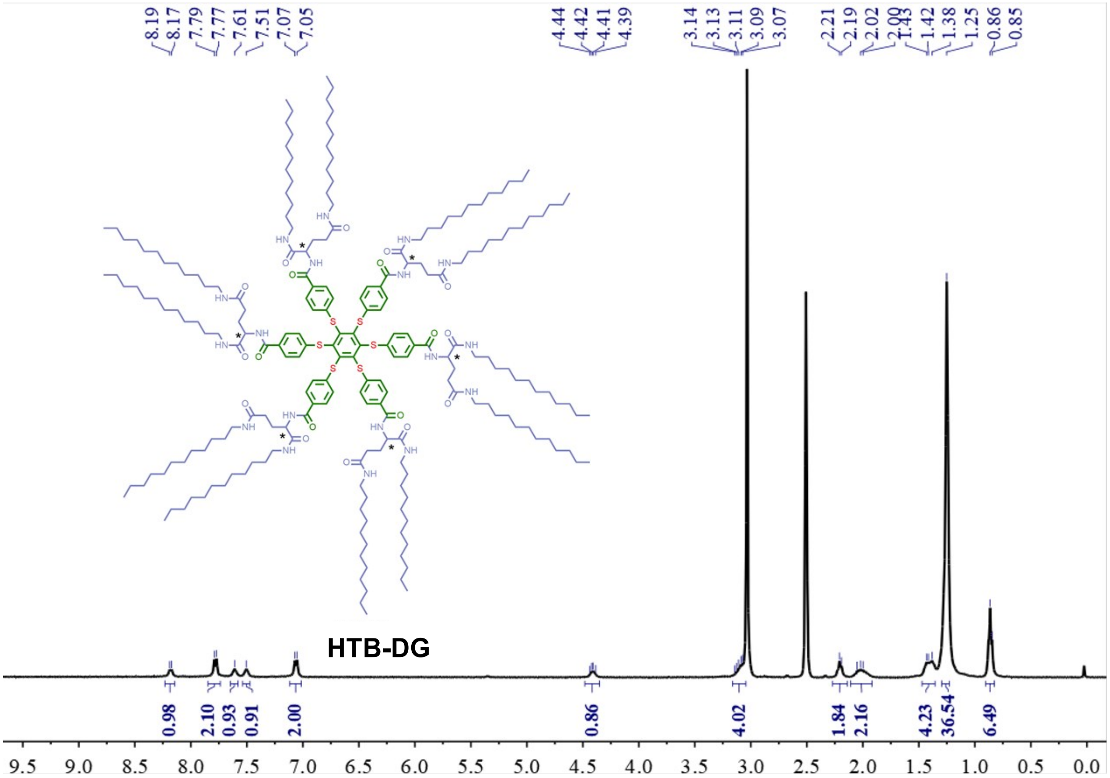

Fig. S7 [1]H NMR spectrum for compound **HTB-DG** (DMSO-d_6, 373 K).

MALDI-TOF MS Spectra for compound HTB-DG:

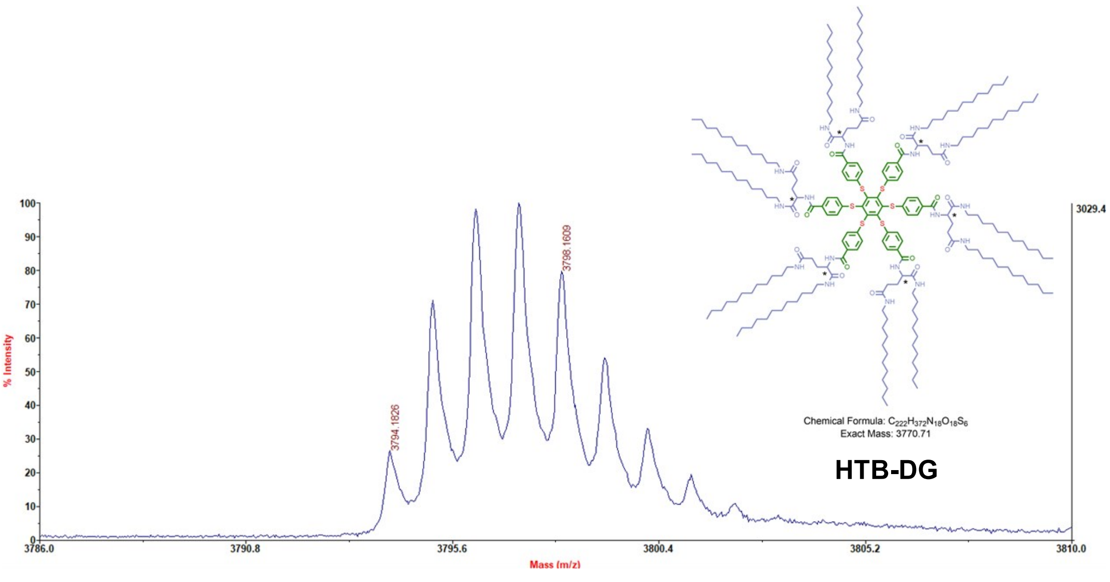

Fig. S8 MALDI-TOF MS Spectrum for compound **HTB-DG**.

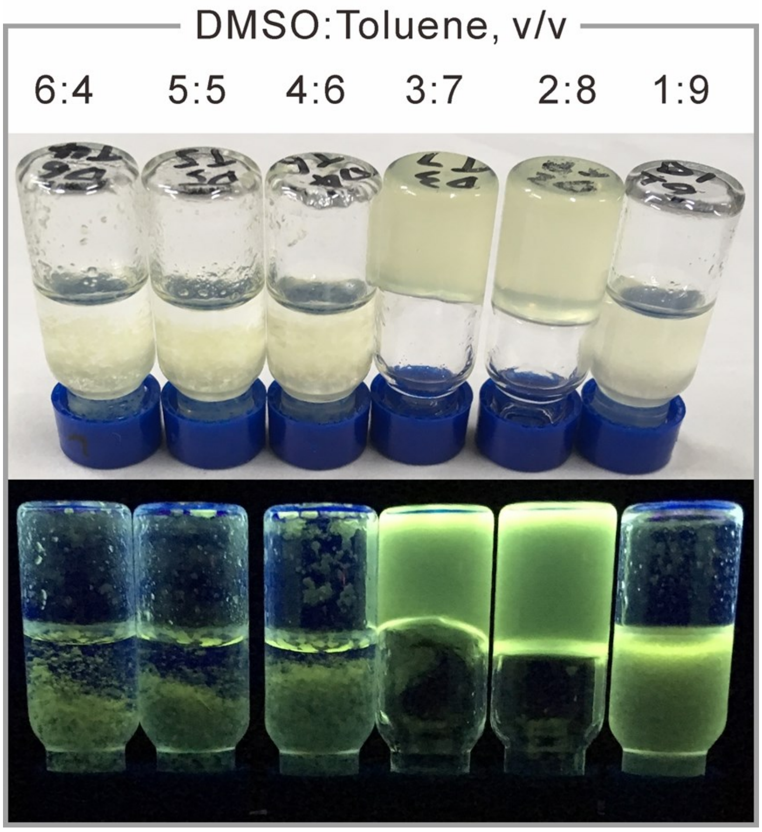

Fig. S9 Solvent ratio test between DMSO and toluene for gel formation. The concentration of **HTB-DG** was 3 mg/mL.

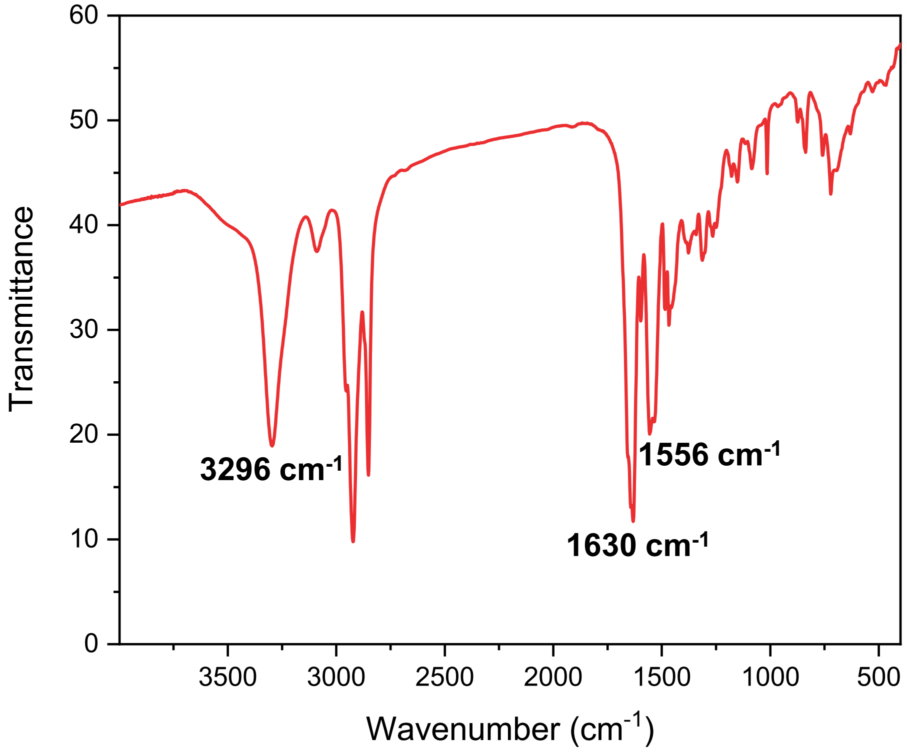

Fig. S10 FTIR spectra of **HTB-DG** xerogel.

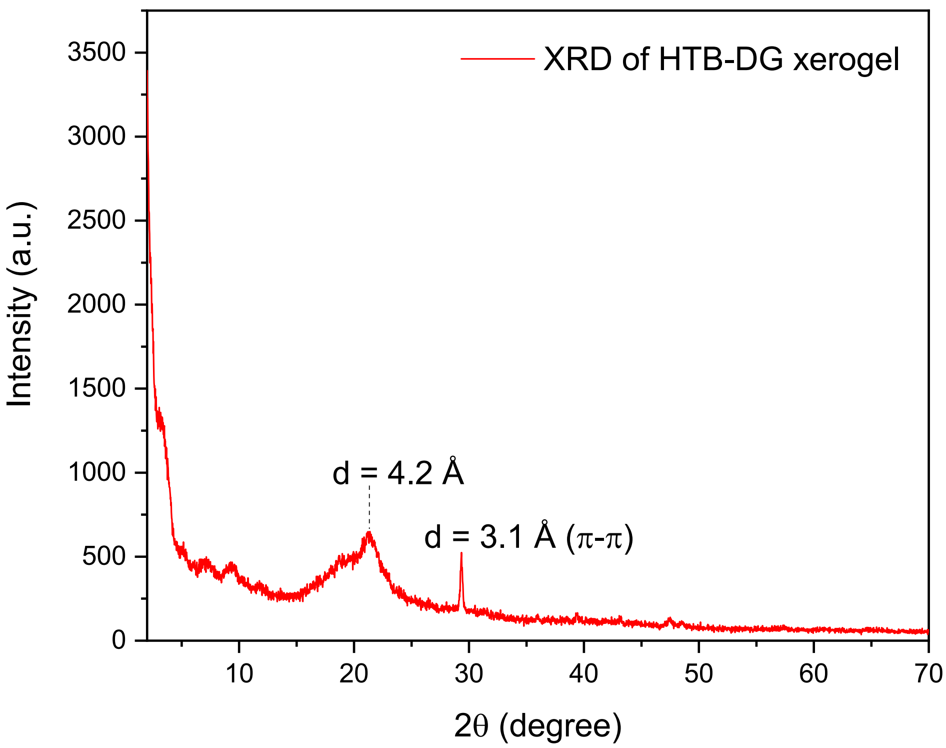

Fig. S11 XRD pattern of **HTB-DG** xerogel.

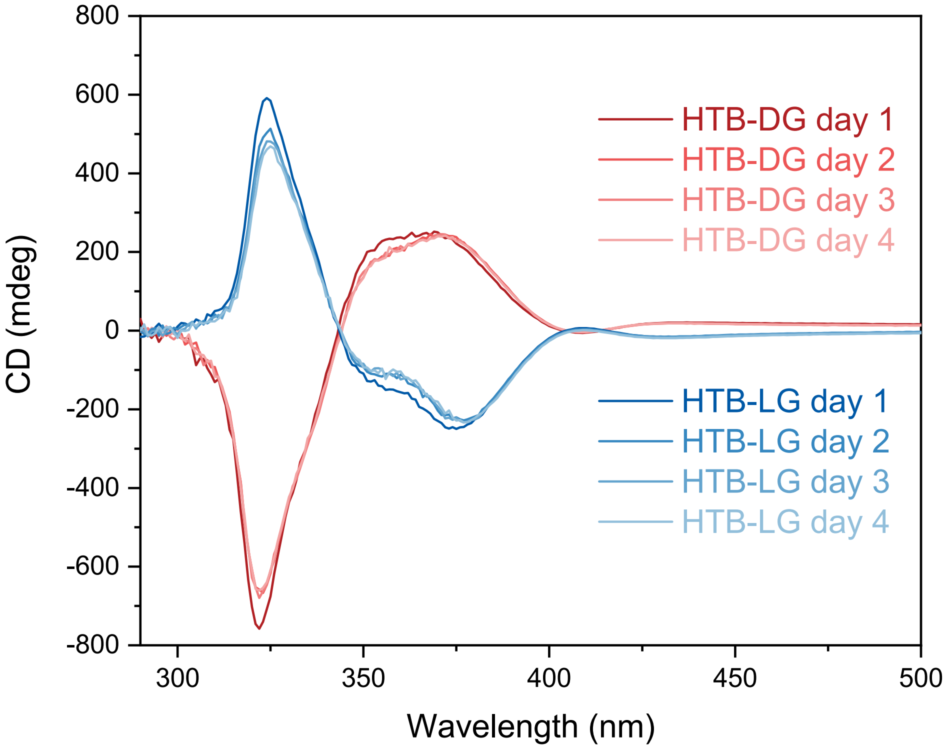

Fig. S12 Time-dependent CD spectra of **HTB-DG** (red lines) and **HTB-LG** (blue lines), concentration: 3 mg/mL, 2 mm cuvette.

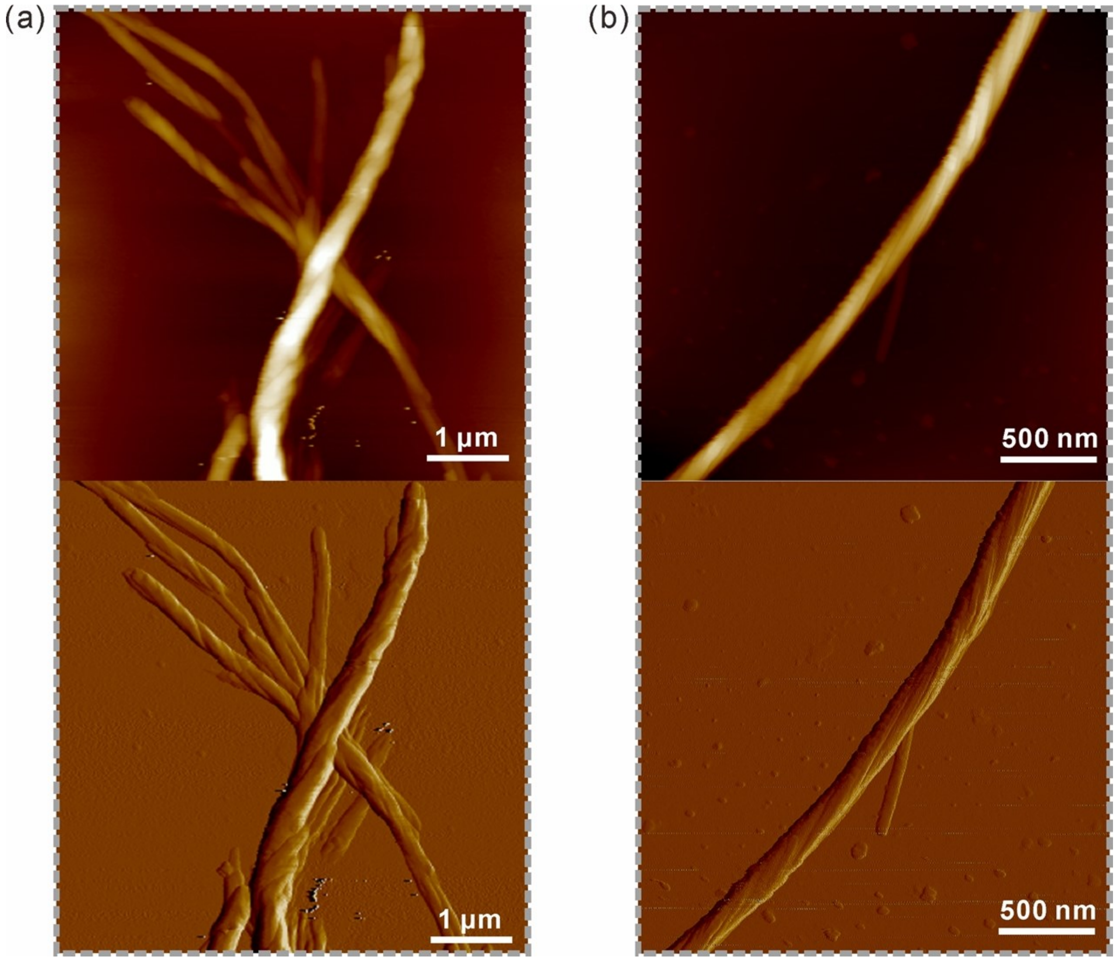

Fig. S13 AFM images of **HTB-DG** (a) and **HTB-LG** (b) xerogels showing helical self-assembly of **HTB-D/LG**.

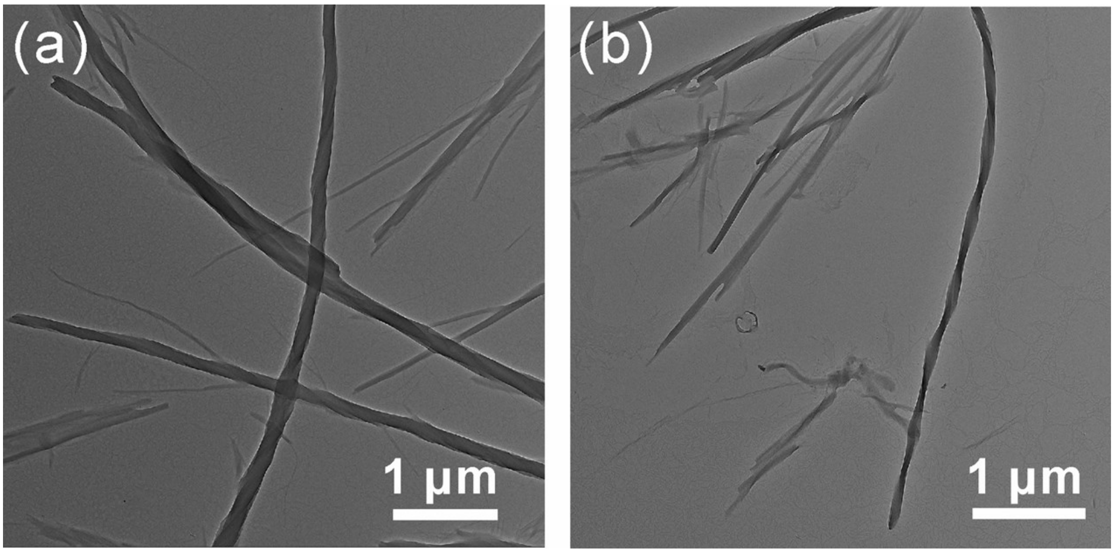

Fig. S14 TEM images of **HTB-DG** (a) and **HTB-LG** (b) xerogels showing helical self-assembly of **HTB-D/LG**.

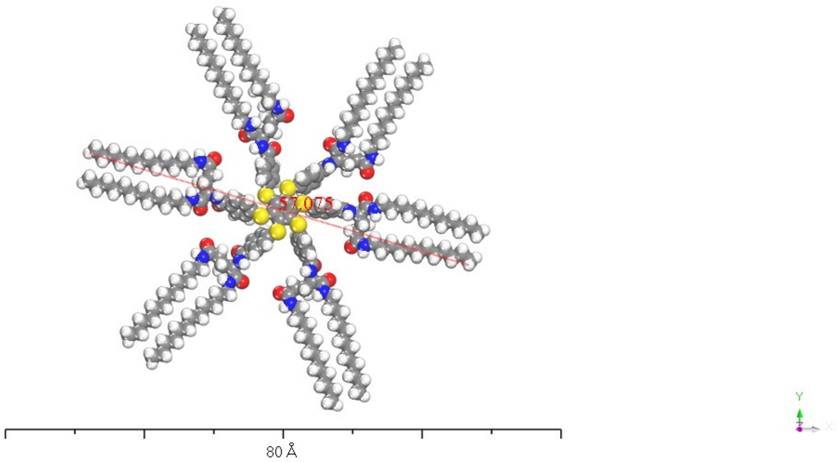

Fig. S15 Estimation of the length of an extended **HTB-D/LG** molecule calculated with Materials Studio package.

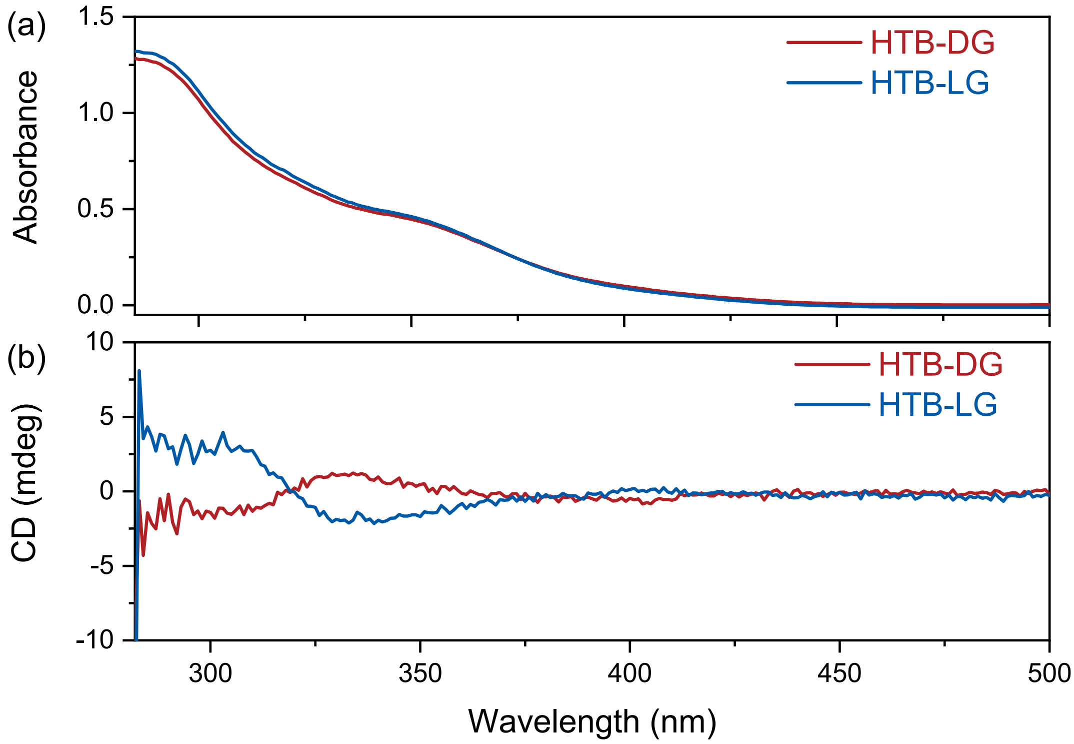

Fig. S16 UV-Vis (a) and corresponding CD (b) spectra of dilute solution of **HTB-DG** (red line) and **HTB-LG** (blue line) in DMSO/toluene (2/8, v/v) mixed solvent, concentration at 15 μM, 1 cm cuvette.

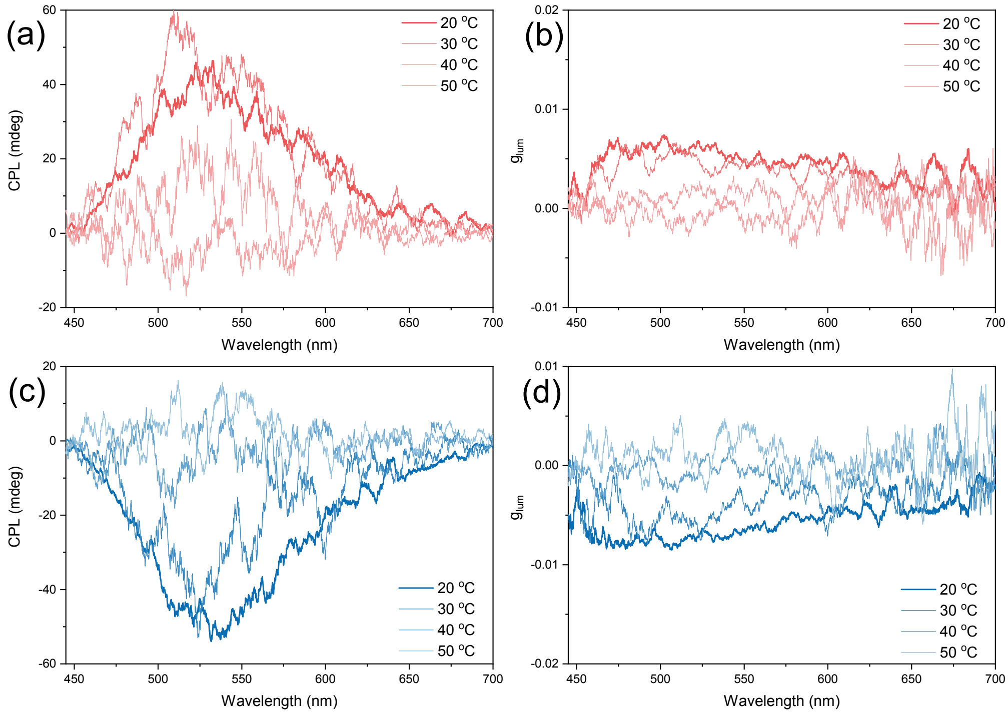

Fig. S17 CPL spectra (a, c) and corresponding g_{lum} (b, d) curves of **HTB-DG** (red lines) and **HTB-LG** (blue lines) organogel depended on temperature (λ_{ex} = 365 nm).

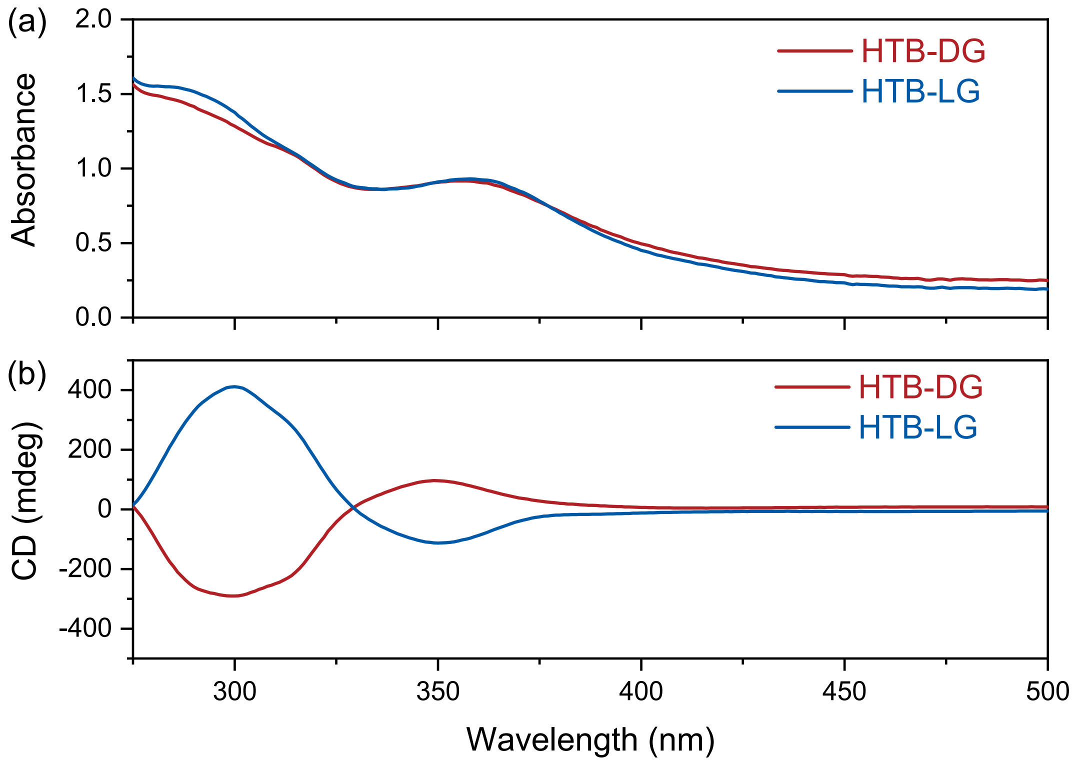

Fig. S18 UV-Vis (a) and corresponding CD (b) spectra of **HTB-DG** (red line) and **HTB-LG** (blue line) organogels, concentration at 10 mg/mL, 0.1 mm cuvette.

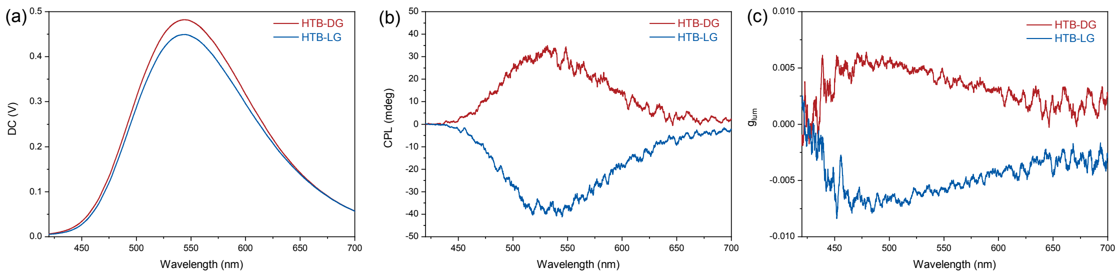

Fig. S19 Photoluminescence (a), CPL spectra (b) and corresponding g_{lum} curves (c) for **HTB-DG** (red line) and **HTB-LG** (blue line) organogels (λ_{ex} = 365 nm), concentration: 10 mg/mL.

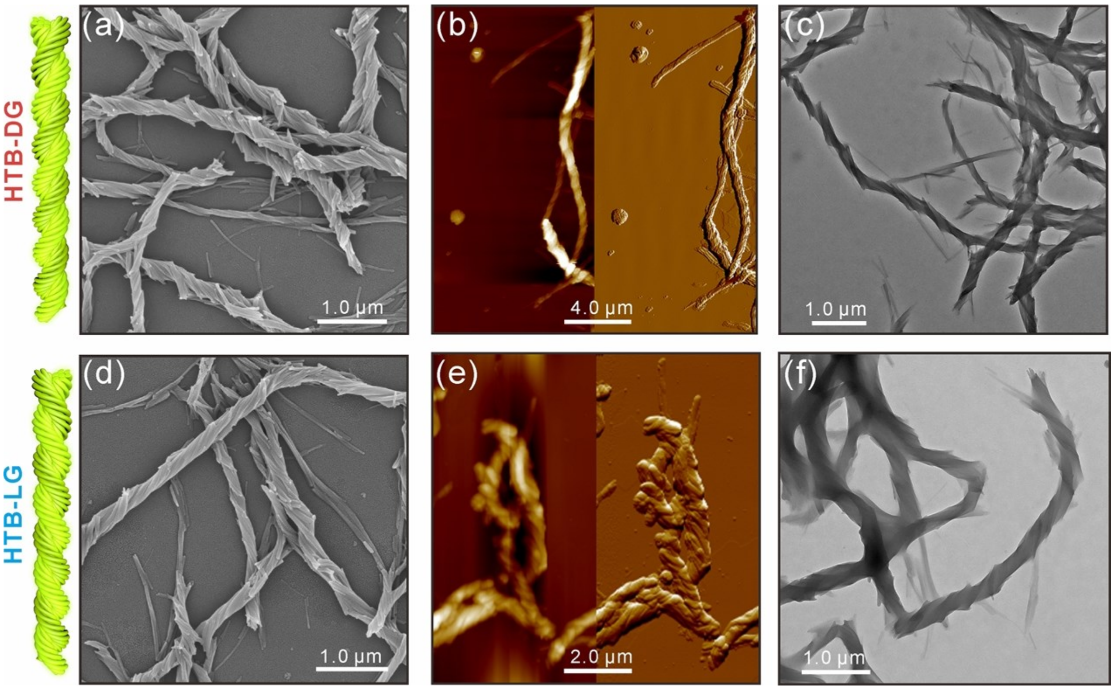

Fig. S20 SEM (a and c), AFM (b and e) TEM (c and f) images for **HTB-DG** (top) and **HTB-LG** (bottom) xerogels, concentration at 10 mg/mL.

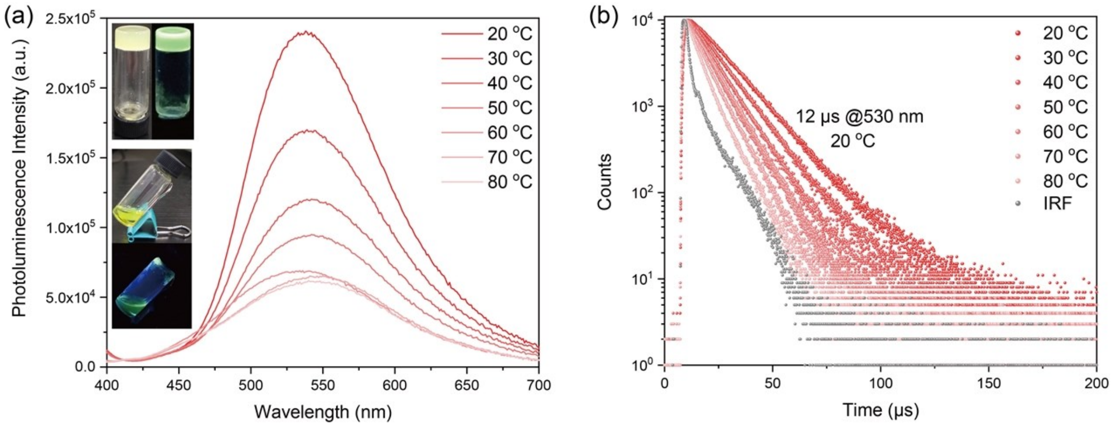

Fig. S21 Temperature-dependent photoluminescence (a) and lifetime (b) spectra of **HTB-DG** organogel (λ_{ex} = 365 nm), concentration at 10 mg/mL. Insets: photographs of **HTB-DG** in gel state (top) and partial sol state (bottom) under ambient light and UV light.

Table S1. Comparison of the chiral response of **THB-D/LG** with reported literatures.

Material	Chiral Response	Other Features	Ref
HTB-D/LG	**thermo ON-OFF CD and CPL response**	**gel, AIE, RTP**	**this work**
S-TPE-Ph-PEA	solvent polarity driven CD and CPL inversion	AIE	Ref S1
DGG/PTPE	stoichiometry-controlled CD and CPL inversion	gel, AIE	Ref S2
cis/trans-TPE-L/D-DGlu	water fraction-controlled CD and CPL inversion in THF/water mixture	AIE	Ref S3
PPA-ACe	thermo-induced helical inversion	Ba^{2+} response	Ref S4
Molecule-2a	thermo-induced helical inversion	encapsulation of C_{60}	Ref S5
PF8	chiral solvent induced CD and CPL; thermo ON-OFF chiropticity	gel	Ref S6
Poly(quinoxaline-2,3-diyl)	solvent-dependent helix inversion	sergeants-and-soldiers effect	Ref S7
Poly-1-H	chiral amine induced macromolecular helicity and chiropticity	helicity memory	Ref S8
(2'S)-(P/M)-3-PHIC	light-controlled chiroptical switch (UV and visible light)	liquid crystalline phase	Ref S9
TPA-SDA	CPL-irradiation-induced helicity	photopolymerization	Ref S10
Poly-R-MPA	helical sense tuning by mono- and divalent metals	dynamic helical polymers	Ref S11
BTACA	vortex mixing-induced CD and CPL	gel	Ref S12

References

S1. Q. Ye, F. Zheng, E. Q. Zhang, H. K. Bisoyi, S. Y. Zheng, D. D. Zhu, Q. H. Lu, H. L. Zhang and Q. Li, *Chem. Sci.*, 2020, **11**, 9989-9993.

S2. P. Li, B. Lu, D. Han, P. Duan, M. Liu and M. Yin, *Chem. Commun.*, 2019, **55**, 2194-2197.

S3. S. Zhang, J. Fan, Y. Wang, D. Li, X. Jia, Y. Yuan and Y. Cheng, *Mater. Chem. Front.*, 2019, **3**, 2066-2071.

S4. F. Wang, C. Zhou, K. Liu, J. Yan, W. Li, T. Masuda and A. Zhang, *Macromolecules*, 2019, **52**, 8631-8642.

S5. Z. Huang, S. K. Kang, M. Banno, T. Yamaguchi, D. Lee, C. Seok, E. Yashima and M. Lee, *Science*, 2012, **337**, 1521-1526.

S6. Y. Zhao, N. A. Abdul Rahim, Y. Xia, M. Fujiki, B. Song, Z. Zhang, W. Zhang and X. Zhu, *Macromolecules*, 2016, **49**, 3214-3221.

S7. Y. Nagata, T. Yamada, T. Adachi, Y. Akai, T. Yamamoto and M. Suginome, *J. Am. Chem. Soc.*, 2013, **135**, 10104-10113.

S8. K. Maeda, M. Nozaki, K. Hashimoto, K. Shimomura, D. Hirose, T. Nishimura, G. Watanabe and E. Yashima, *J. Am. Chem. Soc.*, 2020, **142**, 7668-7682.

S9. D. Pijper, M. G. M. Jongejan, A. Meetsma and B. L. Feringa, *J. Am. Chem. Soc.*, 2008, **130**, 4541-4552.

S10. J. Kim, J. Lee, W. Y. Kim, H. Kim, S. Lee, H. C. Lee, Y. S. Lee, M. Seo and S. Y. Kim, *Nat. Commun.*, 2015, **6**, 6959.

S11. F. Freire, J. M. Seco, E. Quinoa and R. Riguera, *Angew. Chem. Int. Ed.*, 2011, **50**, 11692-11696.

S12. Y. Sang, D. Yang, P. Duan and M. Liu, *Chem. Sci.*, 2019, **10**, 2718-2724.